

Planetary companion candidates around the K giant stars 42 Dra and HD 139357

M.P. Döllinger¹, A.P. Hatzes², L. Pasquini¹, E.W. Guenther², M. Hartmann², and L. Girardi³

¹ European Southern Observatory, Karl-Schwarzschild-Strasse 2, D-85748, Garching bei München, Germany

² Thüringer Landessternwarte Tautenburg, Sternwarte 5, D-07778 Tautenburg, Germany

³ INAF-Osservatorio Astronomico di Padova, Vicolo dell'Osservatorio 5, I-35122 Padova, Italy

Received; accepted

ABSTRACT

Context. For the past 3 years we have been monitoring 62 K giant stars using precise stellar radial velocity (RV) measurements with the 2m Alfred Jensch Telescope of the Thüringer Landessternwarte Tautenburg (TLS).

Aims. To probe the dependence of planet formation on stellar mass by finding planets around intermediate-mass giant stars.

Methods. We present high accuracy RV measurements of the K1.5 III star 42 Dra and the K4 III star HD 139357. The wavelength reference for the RV measurements was provided by an iodine absorption cell placed in the optical path of the spectrograph.

Results. Our measurements reveal that the time series of the radial velocity of 42 Dra shows a periodic variation of 479.1 days with a semiamplitude of $K = 112.5 \text{ ms}^{-1}$. An orbital solution yields a mass function of $f(m) = (5.29 \pm 0.62) \times 10^{-8}$ solar masses (M_{\odot}) and an eccentricity of $e = 0.38 \pm 0.06$. From our template spectra, taken without the iodine cell, we determine a metallicity of -0.46 ± 0.04 dex and a stellar mass of $0.98 \pm 0.06 M_{\odot}$ for this star.

HD 139357 shows periodic RV variations of 1125.7 days with a semiamplitude $K = 159.9 \text{ ms}^{-1}$. An orbital solution yields an eccentricity, $e = 0.10 \pm 0.02$ and mass function, $f(m) = (4.79 \pm 0.57) \times 10^{-7} M_{\odot}$. An iron abundance of -0.13 ± 0.04 dex is obtained, and a stellar mass of $1.31 \pm 0.24 M_{\odot}$ for the parent star is derived. An analysis of the *HIPPARCOS* photometry as well as our H α core flux measurements reveal no variability with the radial velocity period. Keplerian motion is the most likely explanation for the observed radial velocity variations for these stars.

Conclusions. The K giant stars 42 Dra and HD 139357 host extrasolar planets with “minimum masses” of 3.88 ± 0.85 Jupiter masses M_{Jup} and $9.76 \pm 2.15 M_{\text{Jup}}$, respectively.

Key words. star: general - stars: variable - stars: individual: 42 Dra, HD 139357 - techniques: radial velocities - stars: late-type - planetary systems

1. Introduction

Until now more than 250 extrasolar planets around solar-type main-sequence (MS) host stars have been detected via the RV method. Out of these, the number of discovered planetary companions around giant stars is still limited.

Our motivation was to enlarge the regime of stellar masses and characteristics of planet host stars by hunting for planets around K giants to provide us with important clues to the process of planet formation in a still poorly investigated star domain. This is possible because giant host stars tend to be more massive than the solar-mass objects that have been the traditional targets of most planet searches, thus we can probe the dependence of stellar mass on planet formation. In addition these stars are in a different evolutionary status and have different radii and internal structures compared to their MS counterparts. Finally, in contrast to MS stars, the chemical composition of planet host giants shows no preference for metal-rich systems, which has been

interpreted as an evidence for MS pollution (Pasquini et al. 2007).

Hatzes & Cochran (1993) found first indications of sub-stellar companions around giants. They discovered long-period RV variations in three K giants and they proposed two viable hypotheses for these variations in radial velocity: substellar companions or rotational modulation. Recently Hatzes et al. (2006) and Reffert et al. (2006) confirmed that the initial RV variations found by Hatzes & Cochran (1993) in β Gem were in fact due to a planetary companion. Since the first unequivocal discovery of the first extrasolar planet around the K giant HD 137759 (ι Dra) by Frink et al. (2002), several giant stars have been found to host giant planets (Setiawan et al. 2003a, 2003b, 2005; Sato et al. 2003; Hatzes et al. 2005). Currently, a number of groups are actively searching for extrasolar planets around giant stars and this has resulted in a burst of recent discoveries (Sato et al. (2007); Döllinger et al. (2007); Niedzielski et al. (2007); Johnson et al. (2007b); Sato et al. (2008).

2. Observations and data analysis

42 Dra and HD 139357 belong to a star sample observed since February 2004 from the Thüringer Landessternwarte

Send offprint requests to: Michaela P. Döllinger e-mail: mdoellin@eso.org.de

* Based on observations obtained at the 2m Alfred Jensch telescope at the Thüringer Landessternwarte Tautenburg

Tautenburg (*TLS*) as part of the Tautenburg Observatory Planet Search Programme (*TOPS*). This programme uses the coudé échelle spectrograph mounted on the 2m Alfred Jensch telescope. This instrument provides a resolving power of $R = 67,000$ and a wavelength coverage of 4700–7400 Å using the so-called “visual” (VIS) grism mode. The exposure time for both stars ranged between 5–10 minutes depending on the weather conditions and this resulted in a signal-to-noise (S/N) ratio typically greater than 150. Standard CCD data reduction (bias-subtraction, flat-fielding and spectral extraction) was performed using standard *IRAF* routines. An iodine absorption cell placed in the optical path provided the wavelength reference for the velocity measurements.

The RVs were computed using a programme that largely follows the prescription of Butler et al. (1996). It models an observation of the star observed through the cell using a high resolution template spectrum of molecular iodine taken with a Fourier Transform Spectrometer ($R \approx 10^6$) and a template spectrum of the star taken without the iodine cell. The programme takes into account possible changes of the instrumental profile (IP) of the spectrograph by using the procedure outlined in Valenti et al. (1995). Since the IP can also change spatially along a spectral order, these were divided into segments (so-called spectral chunks). About 130 chunks were used in the final analysis. Thus the spatial (and temporal) variations of the IP, which can introduce significant RV errors, were modeled independently for each chunk. Relative wavelength shifts between the iodine and stellar template spectra were computed using a version of the Fahlman & Glaspey (1973) shift-detection algorithm. The RV measurements from all chunks were then combined weighted by the inverse square of the RV standard deviation for each chunk. The internal velocity error of a spectrum is thus the dispersion of all segments used for the analysis. We should note that the measured Doppler shifts are relative to the stellar template and are thus not absolute radial velocities. For the bright K giant stars in our programme we typically achieve a RV precision of about $3\text{--}5 \text{ ms}^{-1}$. This value refers to the internal velocity error.

To exclude rotational modulation as the cause of the RV variations in the 42 Dra and HD 139357 data, we investigated stellar activity in these stars via the $H\alpha$ spectral line. Several studies have shown that the central core of $H\alpha$ forms in the chromosphere. Consequently stars of different chromospheric activity show a different shape (depth and breadth) of the $H\alpha$ core (Pasquini & Pallavicini 1991). It has been widely demonstrated that the $H\alpha$ line can be used as a good “activity indicator” of chromospheric emission (Herbig 1985; Pasquini & Pallavicini 1991; Freire Ferrero et al. 2004). By measuring the variations of the core of $H\alpha$ with respect to the continuum it is therefore possible to investigate the presence and variability of chromospheric active regions.

To determine the chromospheric contribution to the $H\alpha$ profile one has to exclude possible contamination from telluric lines. The normal procedure is to observe so-called “telluric standards” in order to divide out the telluric lines. These are typically early-type, rapidly rotating stars which are observed every night. However, with the spectra of the Tautenburg star sample this subtraction was not done in

this way because early-type stars have very strong balmer lines so using them for taking out telluric lines is not so appropriate. We therefore restricted our $H\alpha$ measurements to the region within $\pm 0.6 \text{ Å}$ of the line center. Two additional spectral regions located at $\pm 50 \text{ Å}$ provided the “continuum” measurement. All of these regions were free of telluric contamination. The $H\alpha$ core measurement was done using a programme that shifts all the spectra to a common rest wavelength and measures the flux ratio of the defined areas (Biazzo 2007, private communication). After running the programme, 74 Dra shows a variability of around 1 % in $H\alpha$ activity. Taking into account that this star was not observed every night in all observing runs this value can only give a hint to the internal error of the measurements. Due to the $H\alpha$ activity of only around 1 % and RV variations at a very low level, which corresponds to the RV precision limit of about $3\text{--}5 \text{ ms}^{-1}$, 74 Dra was used as an internal $H\alpha$ and RV standard. The RV plot of this star is shown in Fig. 1.

The time analysis of the measured $H\alpha$ activity will be discussed in more detail for both *TLS* planet candidates in §3.1 and §3.2.

3. Properties of the stars 42 Dra and HD 139357 and of their planetary companions

3.1. 42 Dra

42 Dra (= HD 170693 = HR 6945 = HIP 90344) has a visual magnitude of $V = 4.83 \text{ mag}$ and is classified in *SIMBAD* as K1.5 III star. As for the *HIPPARCOS* parallaxes, we adopt the values derived by van Leeuwen (2007). The corresponding value is $10.36 \pm 0.20 \text{ mas}$ and this implies an absolute magnitude $M_V = -0.09 \pm 0.04 \text{ mag}$. As demonstrated by van Leeuwen & Fantino (2005) and van Leeuwen (2007), this new reduction has substantially improved the results for the parallaxes of bright stars, with respect to the original values in the ESA catalogue (1997). In the specific case of 42 Dra and HD 139357, although the mean parallax values are close to their previous values, their standard errors are now reduced by factors of about 2.

The stellar parameters of 42 Dra, summarized in Tab. 1 and shown in Fig. 2, were either obtained from the literature or derived from our analysis of the stellar spectra taken without the iodine cell. These high-quality templates allowed us to determine accurate Fe abundances $[\text{Fe}/\text{H}]$, effective temperatures T_{eff} , logarithmic surface gravities $\log g$, and microturbulence velocities ξ .

The results of this analysis for 42 Dra, HD 139357, and the rest of the Tautenburg sample as well as a comparison with previous studies will be presented in more detail in a forthcoming paper.

Metallicity, T_{eff} and absolute V -band magnitude, as derived from *HIPPARCOS* parallaxes, were used as input values to estimate the mass, age, and radius of each programme star by comparing these values to theoretical isochrones using a modified version of Jørgensen & Lindegren’s (2005) method. The result of these method is the total Probability Distribution Function (PDF) for each stellar property (see Fig. 2). The peak of the PDF represents the most probable value of a stellar parameter. A detailed description of the procedure is given in da Silva

Table 1. Stellar parameters of 42 Dra. The properties of the host star are listed in detail.

Spectral type	K1.5III	HIPPARCOS
m_V	4.833 ± 0.005	[mag]
M_V	-0.09 ± 0.04	[mag]
$B - V$	1.19 ± 0.005	[mag]
Parallax	10.36 ± 0.20	[mas]
Distance	96.5 ± 1.9	[pc]
M_* ^(a)	0.98 ± 0.05	[M_\odot]
R_* ^(a)	22.03 ± 1.00	[R_\odot]
Age ^(a)	9.49 ± 1.76	[Gyr]
$T_{\text{eff}}^{(a)}$	4200 ± 70	[K]
[Fe/H] ^(a)	-0.46 ± 0.05	[dex]
$\log g^{(a)}$	1.71 ± 0.05	[dex]
micro turbulence ^(a)	1.6 ± 0.8	[km s^{-1}]

^(a) Döllinger (2008), Döllinger (2009), in preparation

et al. (2006).¹

The time series of our RV measurements (see Tab. 2) of 42 Dra including the orbital fit is plotted in the upper part of Fig. 3. The RV curve of the K giant 42 Dra shows an obvious sinusoidal variation. With the exception of one point (lower right), possibly caused by stellar oscillations, the orbital solution fits the data well. The Lomb-Scargle periodogram of the RV measurements is shown in Fig. 4 and this confirms the presence of a statistically significant peak at a frequency of $\nu = 0.00196 \text{ c d}^{-1}$ ($P = 510.2$ days).

The “False Alarm Probability” (FAP) of the 510-day period peak using the prescription in Scargle (1982) is estimated to be $\approx 2 \times 10^{-7}$. The FAP was also estimated using a “bootstrap randomization technique” (see Kürster et al. 1999). The RV values were randomly shuffled keeping the times fixed and a Lomb-Scargle periodogram calculated for each random data set over the same frequency range shown in Fig. 4. After 200,000 “shuffles” there was no instance of the random periodogram having power larger than the real data set. This confirms that the periodic signal is not due to noise or data sampling.

An orbital solution to the data was made using the general non-linear least squares programme *GaussFit* (McArthur et al. 1994). This resulted in a shorter period of 479.1 ± 6.2 days. The discrepancy between the periods is due to the fact that the Lomb-Scargle programme uses sine functions (i.e. a circular orbit) to find periodic signals in the data. The orbital eccentricity of 42 Dra b is $e = 0.38 \pm 0.06$, so a pure sine wave is not the best fit to the data. Consequently, the Lomb-Scargle periodogram should yield a less reliable period.

All orbital elements are listed in Tab. 3. The corresponding mass function is $f(m) = (5.29 \pm 0.62) \times 10^{-8} M_\odot$. Using our derived stellar mass of $0.98 \pm 0.05 M_\odot$ we calculated a “minimum mass” of $m \sin i = 3.88 \pm 0.85 M_{\text{Jup}}$ for the companion. The line in Fig. 3 shows the orbital solution to the RVs. Fig. 5 shows the phase-folded RV variations and orbital fit.

The RV residuals of 42 Dra are plotted in the lower panel of Fig. 3. A periodogram analysis of the residual

Table 2. Radial velocity measurements for 42 Dra.

JD	RV [m s^{-1}]	σ [m s^{-1}]
2453128.419501	-53.2293	3.90
2453192.524517	-114.8587	4.12
2453193.403201	-126.0224	3.31
2453238.410453	-61.4688	2.84
2453301.329173	50.4884	3.96
2453302.522409	67.6217	5.92
2453303.416619	49.0516	4.46
2453304.252831	59.8095	3.59
2453304.257380	66.2191	6.60
2453419.712262	79.7443	3.23
2453460.616950	98.9271	3.98
2453461.636258	100.0269	3.48
2453476.524540	44.9801	2.88
2453481.567590	66.8865	4.16
2453482.574098	80.2309	4.36
2453483.509160	86.7844	3.04
2453484.527265	29.8126	3.88
2453637.327828	-88.0594	3.52
2453654.447141	-40.0147	4.13
2453655.432914	-59.9776	3.36
2453655.606802	-41.1324	4.49
2453656.461186	-74.5463	3.53
2453656.620815	-65.0586	3.79
2453657.433509	-72.2340	3.77
2453657.609979	-66.5591	4.84
2453899.530210	64.2880	5.17
2453900.481314	88.1803	5.82
2453901.570729	91.9168	4.53
2453904.502606	116.6142	5.73
2453905.551268	129.6684	5.48
2453840.546573	88.7195	3.29
2453995.339307	81.0351	3.00
2454041.290860	-5.0989	3.74
2454047.266968	4.5754	6.48
2454097.222261	-67.5189	4.13
2454136.697758	-139.7974	4.20
2454157.661375	-125.1538	3.45
2454099.192333	-63.6536	4.43
2454099.196558	-66.4595	5.35
2454192.644336	-113.0858	3.29
2454171.672927	-193.1661	3.40
2454309.380979	49.9884	3.23
2454313.374845	86.8409	3.47
2454330.329069	101.4740	3.60
2454337.334089	86.0530	3.15

Table 3. Summary of all orbital parameters for the planetary companion to 42 Dra.

Period[days]	479.1 ± 6.2
$T_{\text{periastron}}$ [JD]	2452757.4 ± 3.7
K [m s^{-1}]	110.5 ± 7.0
$\sigma(\text{O} - \text{C})$ [m s^{-1}]	26.0
e	0.38 ± 0.06
ω [deg]	218.7 ± 10.6
$f(m)$ [M_\odot]	$(5.29 \pm 0.62) \times 10^{-8}$
a [AU]	1.19 ± 0.01

RV data showed no additional significant frequencies in the data. To check, if rotational modulation might be the cause of the observed RV variations we analyzed the *HIPPARCOS* photometry and the $\text{H}\alpha$ activity of 42 Dra. Figs. 6 and 7 show the periodogram of the photometry and the $\text{H}\alpha$ activity, respectively. Neither the *HIPPARCOS*

¹ The present implementation of the PDF method is publicly available via the web interface <http://stev.oapd.inaf.it/param>.

photometry nor the $H\alpha$ data show significant variations at the orbital frequency. From the projected rotational velocity $v \sin i < 1.0 \text{ km s}^{-1}$ (de Medeiros et al. 1996) and the adopted stellar radius, listed in Tab. 1, we have estimated the lower limit of the rotational period. This calculated value of 1113 days is completely different from the orbital period of the planetary companion (see Tab. 3) and confirms that the RV variations are not due to rotational modulation. The typical lifetime of active zones for K giants in general can range between hours to around several hundreds of days.

We note that the sigma of the RVs around the orbital solution is about 26 m s^{-1} , significantly higher than our RV precision. There is also one point which differs significantly from the predicted RV of the orbital solution (lower right in Fig. 3, near the third RV minimum). This scatter most likely arises from stellar oscillations. It is well known that K giant stars show RV variations due to p-mode oscillations with periods ranging from hours to days (e.g. Hatzes & Cochran 1995; de Ridder et al. 2006; Hatzes & Zechmeister 2007). We can use the scaling relations of Kjeldsen & Bedding (1995) to estimate the expected amplitude of such variations. The velocity amplitude for stellar oscillations is predicted to be $v_{osc} = ((L/L_{\odot})/(M/M_{\odot})) \times 23.4 \text{ cm s}^{-1}$ according to Kjeldsen & Bedding (1995) Eq. 7. Using the luminosity, calculated with the spectroscopic effective temperature T_{eff} , the stellar radius R_* , and the stellar mass M_* for 42 Dra results in an amplitude of 22.9 m s^{-1} , consistent with our rms scatter. The characteristic periods for such oscillations are expected to be about 1.7 days according to the Kjeldsen & Bedding scaling relations. Thus, the scatter of the RV data about the orbital solution can be accounted for by stellar oscillations.

3.2. HD 139357

Another exoplanet orbits the slightly metal-poor giant HD 139357 (= HR 5811 = HIP 76311) having the longest period of all Tautenburg planet candidates within this K giant star sample with a period comparable with the duration of our survey. The stellar parameters of this star are summarized in Tab. 4. The PDF diagrams of the stellar parameters are shown in Fig. 8.

The time series of the RV measurements for HD 139357 is shown in the upper panel of Fig. 9. The lower panel shows the RV residuals after subtracting the orbital solution (see below).

The radial velocity data reveal a nearly sine-like long-period variation. A Lomb-Scargle periodogram of the RV data (see Tab. 5) shows significant power corresponding to a period of 1124 days. The FAP of this peak is $\approx 10^{-9}$. We do not show the Lomb-Scargle periodogram as it is readily apparent from Fig. 9 that there are periodic RV variations in this star.

An orbital solution yielded a revised period of 1125.7 days and a slightly eccentric orbit, $e = 0.10 \pm 0.02$. All the orbital elements are listed in Tab. 6 and the orbital solution is shown as a line in Fig. 9. The mass function (see Tab. 6) delivers a “minimum mass” of $m \sin i = 9.76 \pm 2.15 \text{ M}_{\text{Jup}}$ for the substellar companion. It appears that our data window covered slightly more than one orbital period.

The orbital fit to the data is again quite good with an rms scatter of only 14 m s^{-1} . The Kjeldsen & Bedding relations predict an RV amplitude for stellar oscillations of

Table 4. The values of the stellar properties of the planet host star HD 139357 are listed.

Spectral type	K4III	HIPPARCOS
m_V	5.977 ± 0.005	[mag]
M_V	0.61 ± 0.08	[mag]
$B - V$	1.2 ± 0.005	[mag]
Parallax	8.46 ± 0.30	[mas]
Distance	118.2 ± 4.4	[pc]
$M_*^{(a)}$	1.35 ± 0.24	[M_{\odot}]
$R_*^{(a)}$	11.47 ± 0.75	[R_{\odot}]
Age ^(a)	3.07 ± 1.47	[Gyr]
$T_{\text{eff}}^{(a)}$	4700 ± 70	[K]
[Fe/H] ^(a)	-0.13 ± 0.05	[dex]
$\log g^{(a)}$	2.9 ± 0.15	[dex]
micro turbulence ^(a)	1.6 ± 0.8	[km s^{-1}]

^(a) Döllinger (2008), Döllinger (2009), in preparation

13.7 m s^{-1} for this star, consistent with the rms scatter about the orbit. The Lomb-Scargle periodogram after removal of the orbital contribution due to the exoplanet shows no significant periodic signals.

To test if the RV period could arise from rotational modulation we searched for significant frequencies in the 106 data points of the *HIPPARCOS* photometry. Fig. 10 shows the Lomb-Scargle periodogram of the photometry. There is no significant power at the RV frequency.

Fig. 11 shows the Lomb-Scargle periodogram of the $H\alpha$ variations. Again, there is no significant power near the RV frequency.

4. Discussion

Our radial velocity measurements indicate that the K giant stars 42 Dra and HD 139357 host extrasolar giant planets. In the case of 42 Dra, the planet orbit is modestly eccentric which may argue in favour of Keplerian motion. However, it is not highly eccentric as it is the case for ι Dra b. It is still possible for surface structure to produce such a RV curve. The eccentricity argument for HD 139357 is less effective due to its nearly circular orbit. Nevertheless, the lack of variability in the *HIPPARCOS* and the $H\alpha$ data for both stars is more consistent with the planet hypothesis. We caution the reader that the *HIPPARCOS* photometry was not simultaneous with our RV measurements. Thus, we cannot exclude that spots were not present when *HIPPARCOS* observed these stars, but are present now and are causing the RV variations. Anyhow, our $H\alpha$ measurements were made simultaneously to the RV data. We therefore believe that the detected periods of several hundred days in both stars are not due to rotational modulation, but rather to planetary companions.

In the search for exoplanets it is important to investigate, if there are differences between discovered planet-hosting K giants and MS stars and how this different behaviour of MS and giant stars is correlated with the process of planet formation.

The first main difference between MS stars and giants is, that giants on average have a somewhat higher mass than MS stars surveyed for exoplanets. Taking into account that the mass determination in giant stars suffers large uncertainties, the masses of planet-hosting giants vary

Table 5. Radial velocity measurements for HD 139357.

JD	RV[m s ⁻¹]	σ [m s ⁻¹]
2453051.723680	54.6949	6.84
2453123.549508	23.4178	6.88
2453124.560375	25.5474	6.88
2453128.560125	10.4159	6.7
2453189.548814	-10.5455	6.26
2453193.487180	-35.7487	7.86
2453234.514517	-40.2842	18.80
2453234.519540	-67.3711	8.47
2453238.371353	-60.0982	6.65
2453301.406657	-126.0780	8.43
2453303.224983	-90.0338	8.63
2453460.552279	-161.6434	7.96
2453461.541417	-167.5064	7.89
2453477.430919	-158.2766	6.81
2453477.445942	-157.2085	5.34
2453481.533417	-158.9196	8.19
2453483.475855	-161.8257	6.28
2453484.493369	-167.2390	7.72
2453544.479554	-134.8390	6.68
2453636.302387	-52.2132	7.41
2453654.401421	-12.7092	8.23
2453655.391132	-42.2359	7.65
2453656.423032	-31.6170	8.77
2453657.388311	-21.9815	8.18
2453899.494524	152.8739	7.31
2453900.458972	131.9554	6.75
2453901.517734	166.2499	7.65
2453904.481294	162.0390	7.47
2453905.504617	166.7464	7.09
2453905.543261	183.4914	7.29
2453840.461750	137.6694	6.71
2453840.539181	138.8760	7.12
2453861.471208	86.9460	9.61
2453873.541128	150.0565	10.28
2453863.414579	126.4515	10.88
2453995.390302	173.9031	15.99
2454047.208226	125.9478	7.16
2454099.209659	128.9890	11.13
2454099.213884	117.1589	11.36
2454099.213884	117.1589	11.36
2454192.660473	71.3733	6.05
2454171.653737	85.5406	6.30
2454245.373811	19.2284	6.51
2454309.388842	-8.9711	8.15
2454309.393113	-30.9135	6.67
2454317.509380	-16.7829	6.31
2454330.333603	-53.7373	7.56
2454337.326745	-35.3002	6.24
2454338.350758	-60.2710	7.29

between ~ 0.9 and $\sim 3 M_{\odot}$ (da Silva et al. 2006; Döllinger 2008), while those of MS stars are between ~ 0.75 and $\sim 1.5 M_{\odot}$.

Another difference between MS and giant stars is their large radius in comparison to MS stars. To study this point we used the stars of the *TLS* programme and the previous southern giant survey carried out with the Fiber-fed Extended Range Optical Spectrograph (*FEROS*) by Setiawan et al. (2004a, 2005). The *FEROS* and *TLS* giants have radii on average about 10 times larger than solar stars (da Silva et al. 2006; Döllinger et al. 2008b). High metallicity could favour the migration of the planets towards short-period systems; in this case, metal-rich stars would have many more short-period planets than

Table 6. All orbital parameters for the companion to the K giant host star HD 139357.

Period[days]	1125.7 ± 9.0
$T_{\text{periastron}}[\text{JD}]$	2452466.7 ± 3.2
$K[\text{m s}^{-1}]$	161.2 ± 3.2
$\sigma(\text{O} - \text{C})[\text{m s}^{-1}]$	14.14
e	0.10 ± 0.02
$\omega[\text{deg}]$	235.4 ± 10.6
$f(m)[M_{\odot}]$	$(4.79 \pm 0.57) \times 10^{-7}$
$a[\text{AU}]$	2.36 ± 0.02

metal-poor stars. These planets would be detected among the MS stars, but no longer around the giants because the star, enlarging its radius as it evolves, would have swallowed up them. It was noted in Pasquini et al. (2007) (see their Fig. 1) that the metallicity distribution is very different for giants than for dwarfs hosting planets with comparable long orbital periods, that is, excluding those with short orbits. This would indicate that the effects of migration, even if present, cannot explain the observed trend.

The third difference has been derived from our high resolution spectra. The abundance analysis for 42 Dra shows that this star is the most metal-poor of our Tautenburg sample with $[\text{Fe}/\text{H}] = -0.46 \pm 0.05$ dex. However, it is less metal-poor than HD 13189 (Hatzen et al. 2005) with a value of -0.58 ± 0.05 dex and also less metal-poor than HD 47536 (Setiawan et al. 2003a) with a value of -0.68 ± 0.05 dex. This is interesting because MS stars hosting exoplanets tend to be metal-rich compared to stars that do not possess exoplanets (Santos et al. 2004). Other authors (Schuler et al. 2005; da Silva et al. 2006) have also found evidence that planet-hosting giant stars are metal-poor. Pasquini et al. (2007) have shown that this characteristic holds for most giants hosting planets. We also note that Cochran et al. (2007) found a giant planet around the MS star HD 155358 with a metallicity of $[\text{Fe}/\text{H}] = -0.68$ dex. The basic question is if the increased metallicity of planet hosting MS stars enhances planet formation, or whether the high metallicity is caused by the presence of a planetary system. The correlation with the metallicity can thus be either cause or effect. The observed metallicity distribution of both types of host stars of extrasolar planetary systems should be thus very helpful to choose between the two most popular planet formation mechanisms: core accretion and gravitational instability.

In the first case, favoured by the core accretion scenario (Pollack et al. 1996), the stars should be overmetallic down to their center. Results on MS stars obtained by several groups (Fischer & Valenti 2005; Ecuivillon et al. 2006) favour this primordial scenario, where stars are born in high metallicity clouds. In the second case the higher values for the metallicity are not primordial, but possibly due to the pollution of the convective envelope of the star by the infall of planets and/or planetesimals as well as comets or asteroids (Gonzalez 1998; Laughlin & Adams 1997; Gonzalez 2001; Murray et al. 1998; Quillen & Holman 2000) onto the star. This pollution can be also caused by the total inward migration of a planet onto the parent star as well as the transfer of material from the disc to the host star as a result of the migration process (Goldreich & Tremaine 1980; Lin et al. 1996) or to the

break-up and infall of one or more planets in multiple systems onto the surface of the star due to gravitational interactions (Rasio & Ford 1996) with other companions. If the star was polluted by the debris of the planetary system, then only the external layers of the atmosphere of the star were affected by this pollution (Laughlin & Adams 1997). Assuming this scenario, the difference in the mass of the convective envelope between MS stars and giants would explain why the metal excess observed in MS stars is not observed among evolved stars. The reason is that the metal excess produced by this pollution, while visible in the thin atmospheres of solar-type stars, is completely diluted in the extended, massive atmospheres of the giants. The hypothesis of pollution in combination with the convective envelope of evolved stars is a possible explanation for the different metallicities between MS and giant stars, but other reasons like a scenario which includes strong differences in planet formation with stellar mass and possibly planet migration is plausible and cannot be excluded.

5. Conclusions

We have found hints that the K giant stars 42 Dra and HD 139357 host extrasolar planets. Both host stars are metal-poor and seem to indicate, in contrast to what is observed among MS stars, that giant planets around giant stars do not favour metal-rich stars.

Acknowledgements. We are grateful to the user support group of the Alfred Jensch telescope: B. Fuhrmann, J. Haupt, Chr. Högner, U. Laux, M. Pluto, J. Schiller, and J. Winkler. We are also grateful to K. Biazzo for the IDL² programme extracting the chromospheric contribution. This research made use of the SIMBAD database, operated at CDS, Strasbourg, France.

References

- Butler, R.P., Marcy, G.W., Williams, E., McCarthy, C., Dosanji, P., & Vogt, S.S., 1996, *PASP* 108, 500
- Cochran, W.D., Endl, M., Wittenmyer, R.A., Bean, J.L. 2007, *AJ*, 665, 1407
- da Silva, L., Girardi, L., Pasquini, L., Setiawan, J., von der Lüh, O., de Medeiros, J.R., Hatzes, A., Döllinger, M.P., and Weiss, A. 2006, *A&A*, 458, 603
- de Ridder, J., Barban, C., Carrier, F., Mazumdar, A., Eggenberger, P., Aerts, C., Deruyter, S., Vanautgaerden, J. 2006, *A&A*, 448, 689
- Döllinger, M.P., Hatzes, A.P., Pasquini, L., Guenther, E.W., Hartmann, M., Girardi, L., and Esposito, M. 2007, *A&A*, 472, 649
- Döllinger, M.P. 2008, PhD, LMU München, accepted
- Döllinger, M.P. 2009, in preparation
- Ecuivillon, A., Israelian, G., Santos, N.C., Mayor, M., and Gilli, G. 2006, *A&A*, 449, 809
- ESA, 1997, *yCat*.1239...OE
- Fahlman, G.G., and Glaspey, J.W. 1973 in *Astronomical Observations with Television Type Sensors*, ed. J.W. Glaspey, and G.A.H. Walker, (Vancouver, B.C.: Inst. of Astronomy and Space Science), 347
- Fischer, D., & Valenti, J. 2005, *ApJ*, 622, 1102
- Freire Ferrero, R., Frasca, A., Marilli, E., and Catalano, S. 2004, *A&A*, 413, 657
- Frink, S., Mitchell, D.S., Quirrenbach, A., Fischer, D.A., Marcy, G.W., and Butler, R. P. 2002, *ApJ*, 576, 478
- Goldreich, P., and Tremaine, S. 1980, *ApJ*, 241, 425
- Gonzalez, G. 1998, *A&A*, 334, 221
- Gonzalez, G., Laws, C., Tyagi, S., and Reddy, B.E. 2001, *AJ*, 121, 432
- Hatzes, A.P., and Cochran, W.D. 1993, *ApJ*, 413, 339
- Hatzes, A.P., and Cochran, W.D. 1995, *ApJ*, 452, 401
- Hatzes, A.P., Guenther, E.W., Endl, M., Cochran, W.D., Döllinger, M.P., and Bedalov, A. 2005, *A&A*, 437, 743
- Hatzes, A.P., Cochran, W.D., Endl, M., Guenther, E.W., Saar, S.H., Walker, G.A.H., Yang, S., Hartmann, M., Esposito, M., Paulson, D.B., and Döllinger, M.P. 2006, *A&A*, 457, 335
- Hatzes, A.P., & Zechmeister, M. 2007, *AAS*, 211, 2104
- Herbig, G.H. 1985, *ApJ*, 289, 269
- Jørgensen, and B.R., Lindegren, L. 2005, *A&A*, 436, 127
- Johnson, J.A., Butler, R.P., Marcy, G.W., Fischer, D.A., Vogt, S.S., Wright, J.T., and Peek, K.M.G. 2007a, *ApJ*, 670, 833
- Johnson, J.A., Marcy, G.W., Fischer, D.A., Wright, J.T., Reffert, S., Kregenow, J.M., Williams, P.K.G., and Peek, K.M.G. 2007b, *arXiv0711.4367J*
- Kjeldsen, H. & Bedding, T.R. 1995, 293, 87
- Kürster, M., Schmitt, J.H.M.M., Cutispoto, G. & Dennerl, K. 1997, *A&A*, 320, 831
- Laughlin, G., and Adams, F.C. 1997, *ApJ*, 491, 51
- Lin, D.N.C., Bodenheimer, P., and Richardson, D.C. 1996, *Natur*, 380, 606
- McArthur, B., Jefferys, W., and McCartney, J. 1994, *AAS*, 184, 2804
- Murray, N., Hansen, B., Holman, M., and Tremaine, S. 1998, *Sci*, 279, 69
- Niedzielski, A., Konacki, M., Wolszczan, A., Nowak, G., Maciejewski, G., Gelino, C.R., Shao, M., Shetrone, M., and Ramsey, L.W. 2007, *ApJ*, 669, 1354
- Pasquini, L., and Pallavicini, R. 1991, *A&A*, 251, 199
- Pasquini, L., Döllinger, M. P., Weiss, A., Girardi, L., Chavero, C., Hatzes, A. P., da Silva, L., Setiawan, J. 2007, *A&A*, 473, 979
- Pollack, J.B., Hubickyj, O., Bodenheimer, P., Lissauer, J.J., Podolak, M., and Greenzweig, Y. 1996, *Icarus*, 124, 62
- Quillen, A.C., and Holman, M. 2000, *AJ*, 119, 397
- Rasio, F.A., and Ford, E.B. 1996, *Sci* 274, 954
- Reffert, S., Quirrenbach, A., Mitchell, D.S., Albrecht, S., Hekker, S., Fischer, D.A., Marcy, G.W., and Butler, R.P. 2006, *ApJ*, 652, 661
- Santos, N.C., Israelian, G., and Mayor, M. 2004, *A&A*, 415, 1153
- Sato, B., Ando, H., and Kambe, E. 2003, *ApJ* 597, L157
- Sato, B., Izumiura, H., Toyota, E., Kambe, E., Takeda, Y., Masuda, S., Omiya, M., Murata, D., Itoh, Y., Ando, H., and 4 coauthors 2007, *ApJ*, 661, 527
- Sato, B., Izumiura, H., Toyota, E., Kambe, E., Ikoma, M., Omiya, M., Masuda, S., Takeda, Y., Murata, D., Itoh, Y. 2008, *arXiv0802.2590*
- Scargle, J.D. 1982, *ApJ*, 263, 835
- Setiawan, J., Hatzes, A.P., von der Lüh, O., Pasquini, L., Naef, D., da Silva, L., Udry, S., Queloz, D., and Girardi, L. 2003a, *A&A*, 397, 1151
- Setiawan, J., Pasquini, L., da Silva, L., von der Lüh, O., and Hatzes, A. 2003b, *A&A*, 398, L19
- Setiawan, J., Rodmann, J., da Silva, L., Hatzes, A.P., Pasquini, L., von der Lüh, O., de Medeiros, J.R., Döllinger, M.P., and Girardi, L. 2005, *A&A*, 437, L31
- Schuler, S.C., Kim, J.H., Tinker, M.C., Jr., King, J.R., Hatzes, A.P., and Guenther, E.W. 2005, *ApJ*, 632, 131
- Valenti, J.A., Butler, R.P., and Marcy, G.W. 1995, *PASP*, 107, 966
- van Leeuwen, F. & Fantino, E. 2005, *A & A* 438, 791
- van Leeuwen, F. 2007, *&A* 474, 653

List of Objects

‘42 Dra, HD 139357’ on page 1

² IDL (Interactive Data Language) is a data visualization and analysis platform.

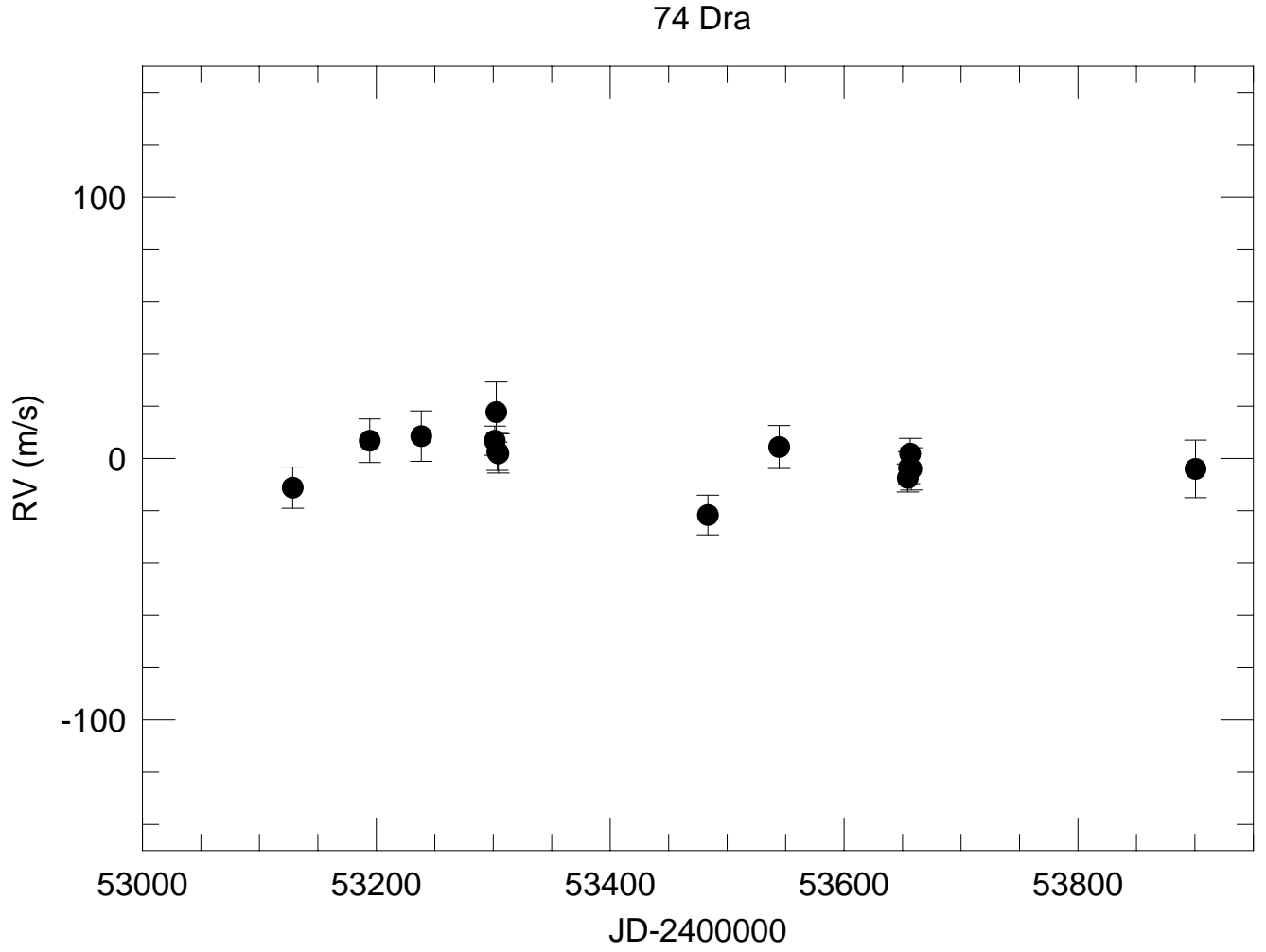


Fig. 1. RV measurements of the target star 74 Dra. Given a strict RV limit of $< 10 \text{ ms}^{-1}$ this star is per definition “constant” and used as RV standard.

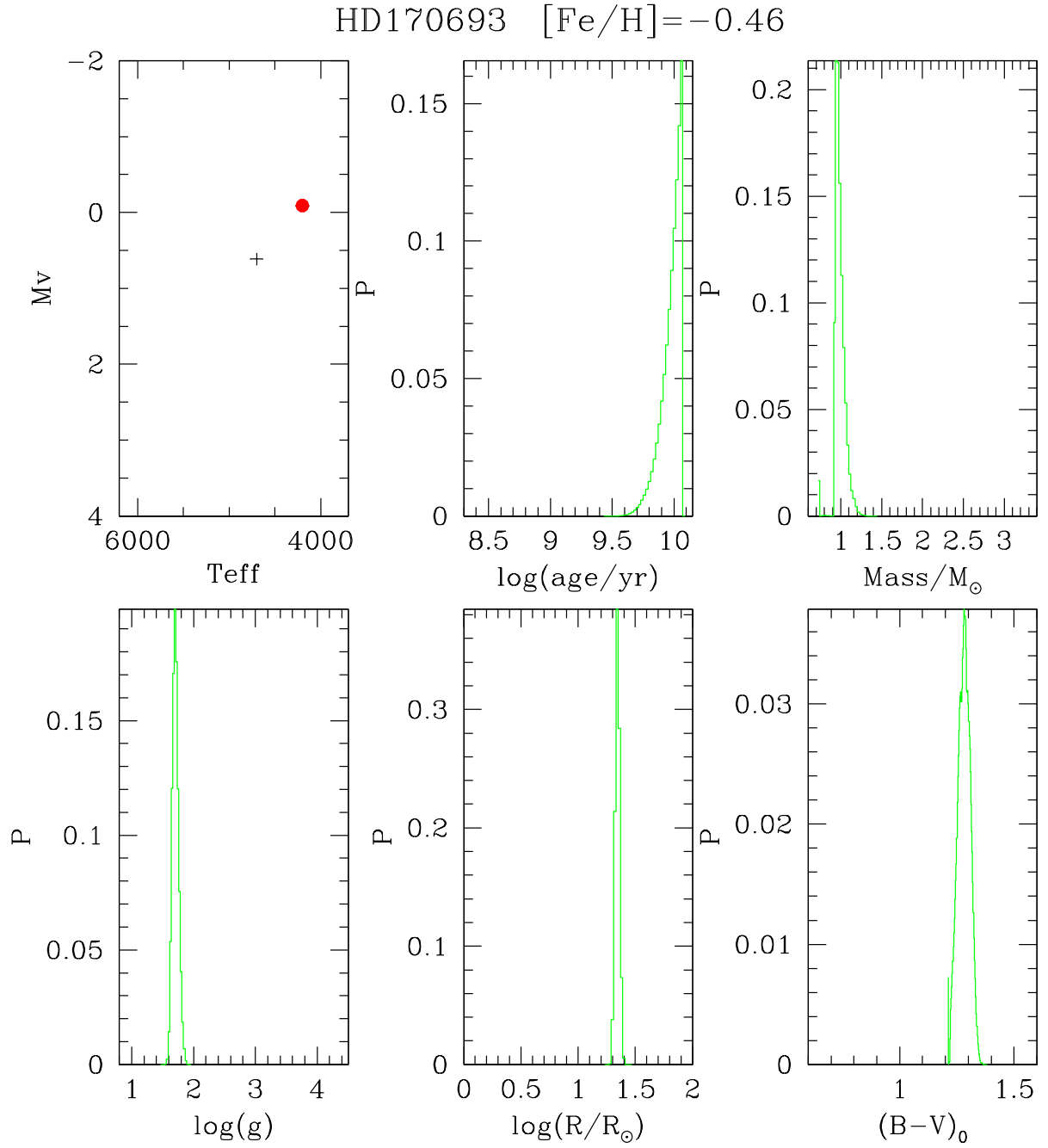


Fig. 2. Diagram of the total Probability Distribution Function (PDF) of the stellar parameters for 42 Dra. The peak of the PDF represents the most probable value of each stellar property.

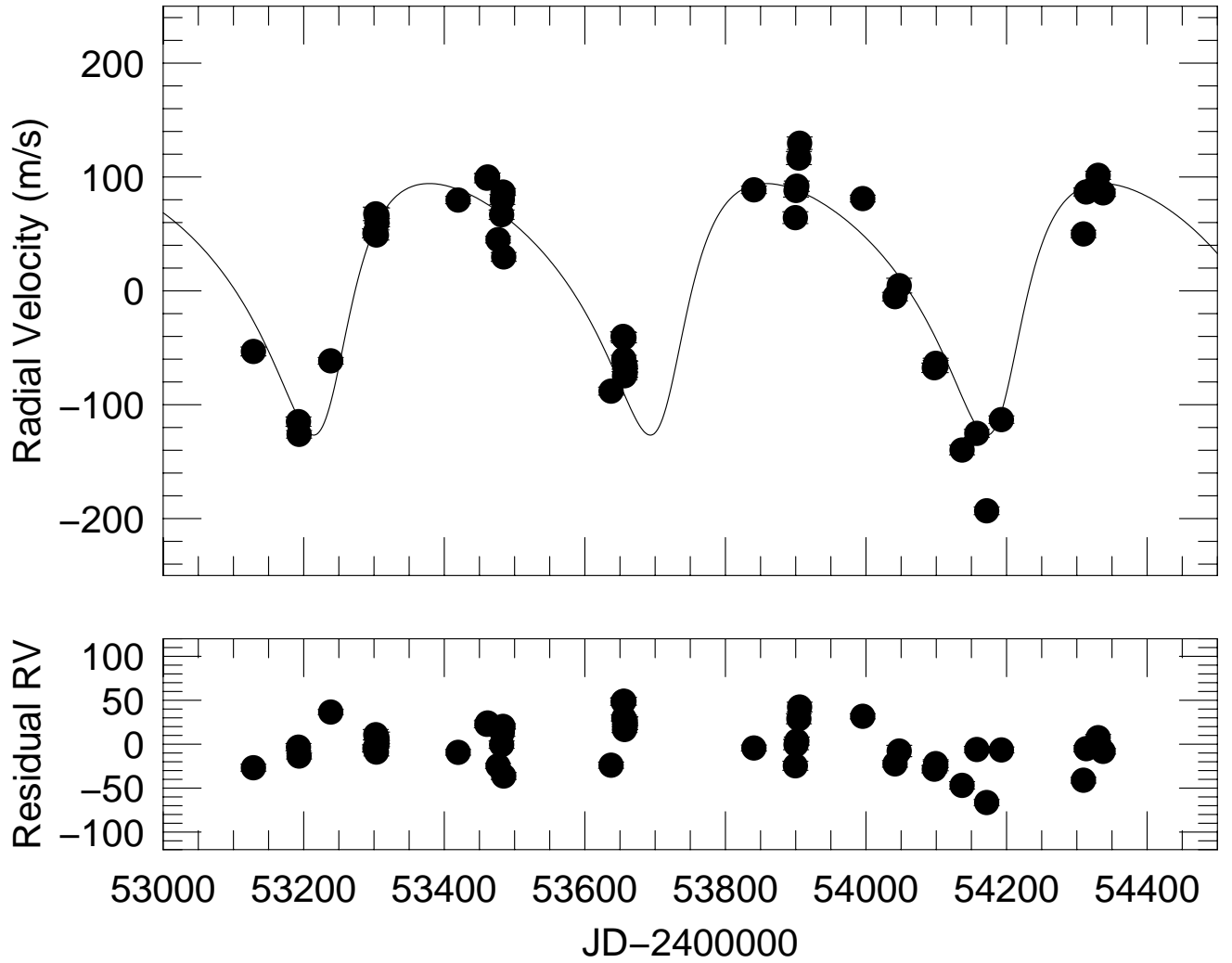


Fig. 3. Radial velocity measurements for 42 Dra (top). The solid line is the orbital solution. The RV residuals (lower) seem to contain short-period variations. However the Lomb-Scargle periodogram shows no significant frequency.

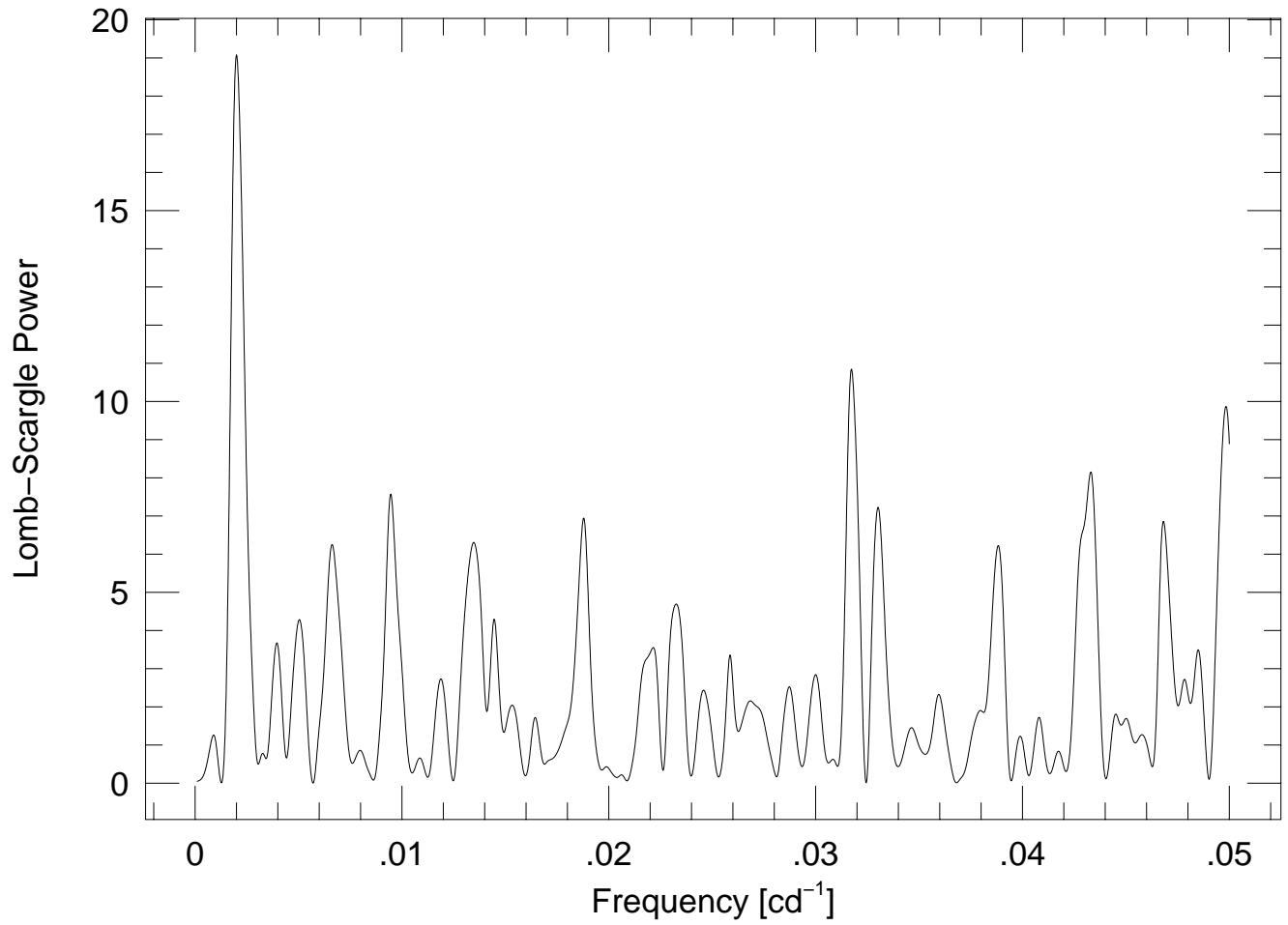


Fig. 4. Lomb-Scargle periodogram for 42 Dra. There is a very high peak with the scargle power 19.0 at a frequency $\nu = 0.00196 \text{ cd}^{-1}$ corresponding to a period of 510.2 days.

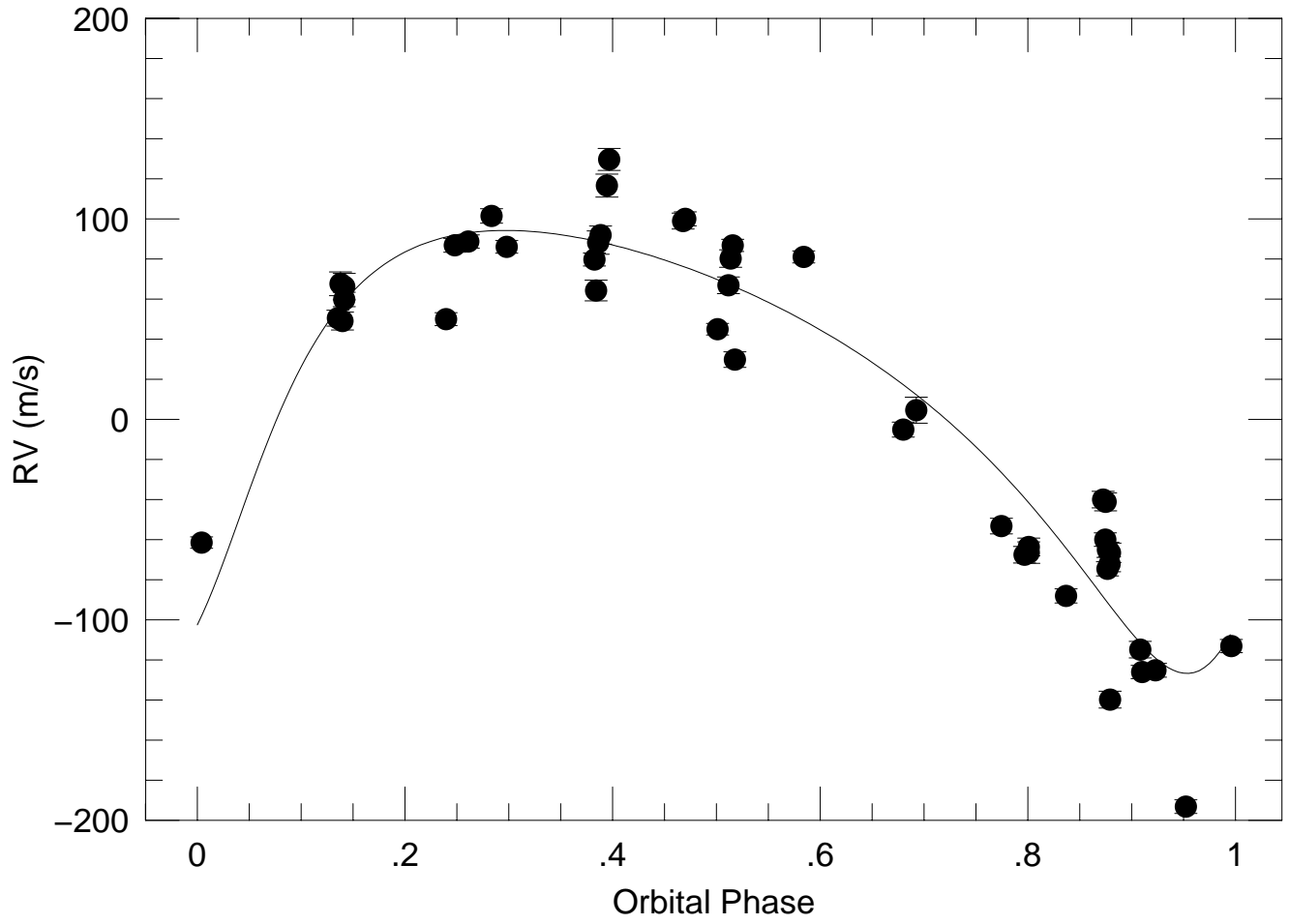


Fig. 5. Radial velocity measurements for 42 Dra phased to the orbital period.

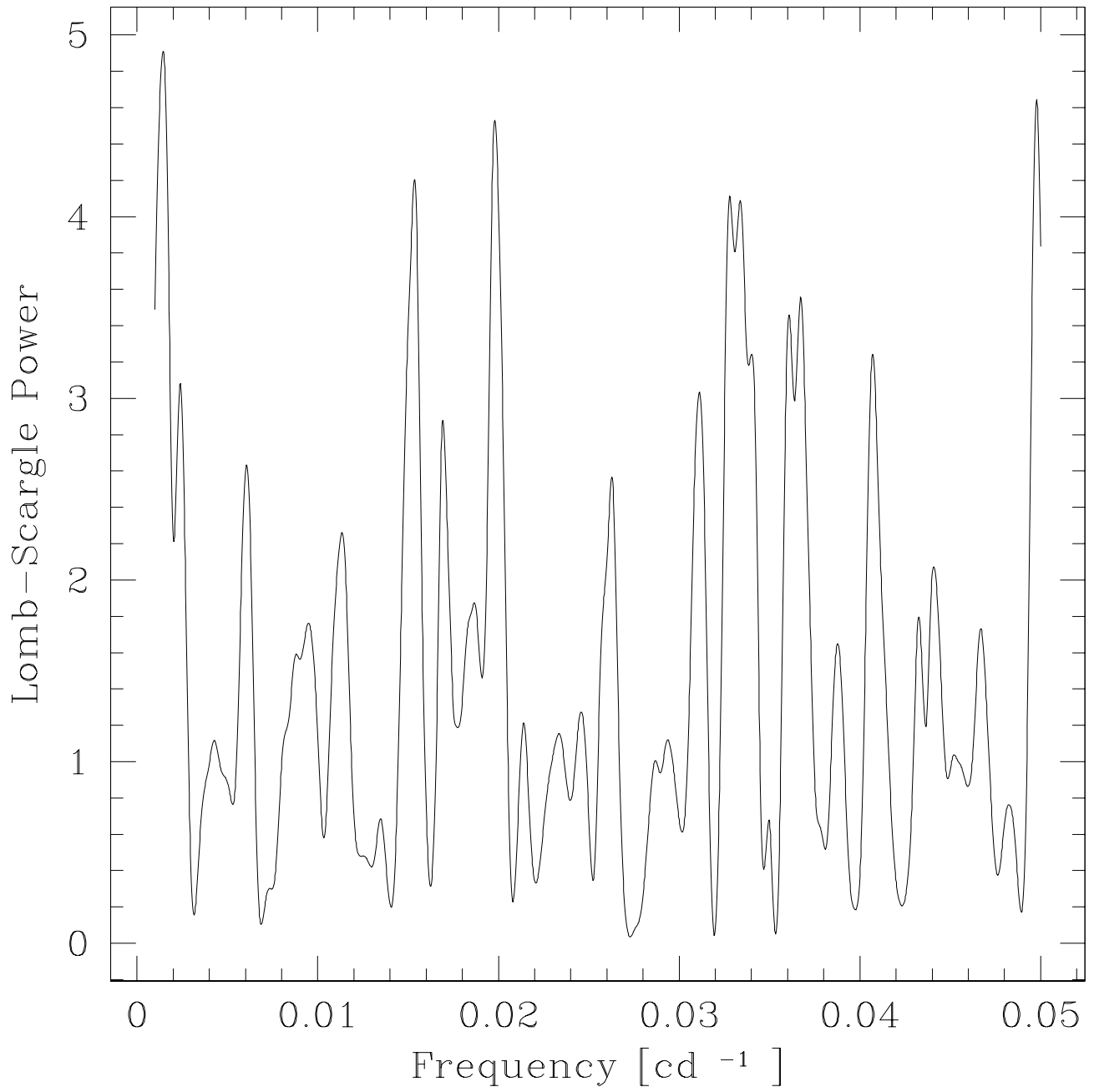


Fig. 6. Lomb-Scargle periodogram of the *HIPPARCOS* photometry for 42 Dra.

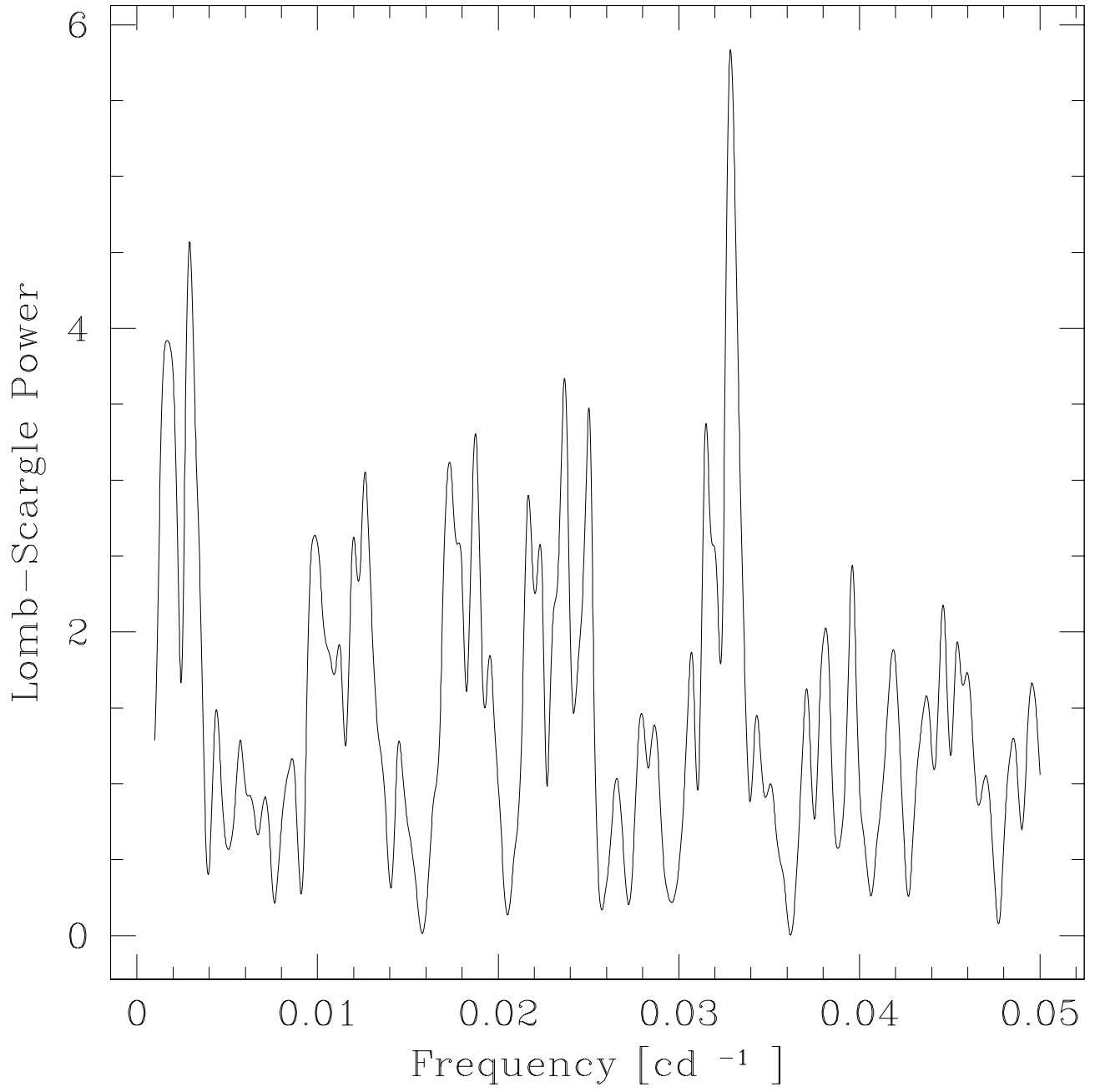


Fig. 7. Lomb-Scargle periodogram of the 42 Dra H α variations.

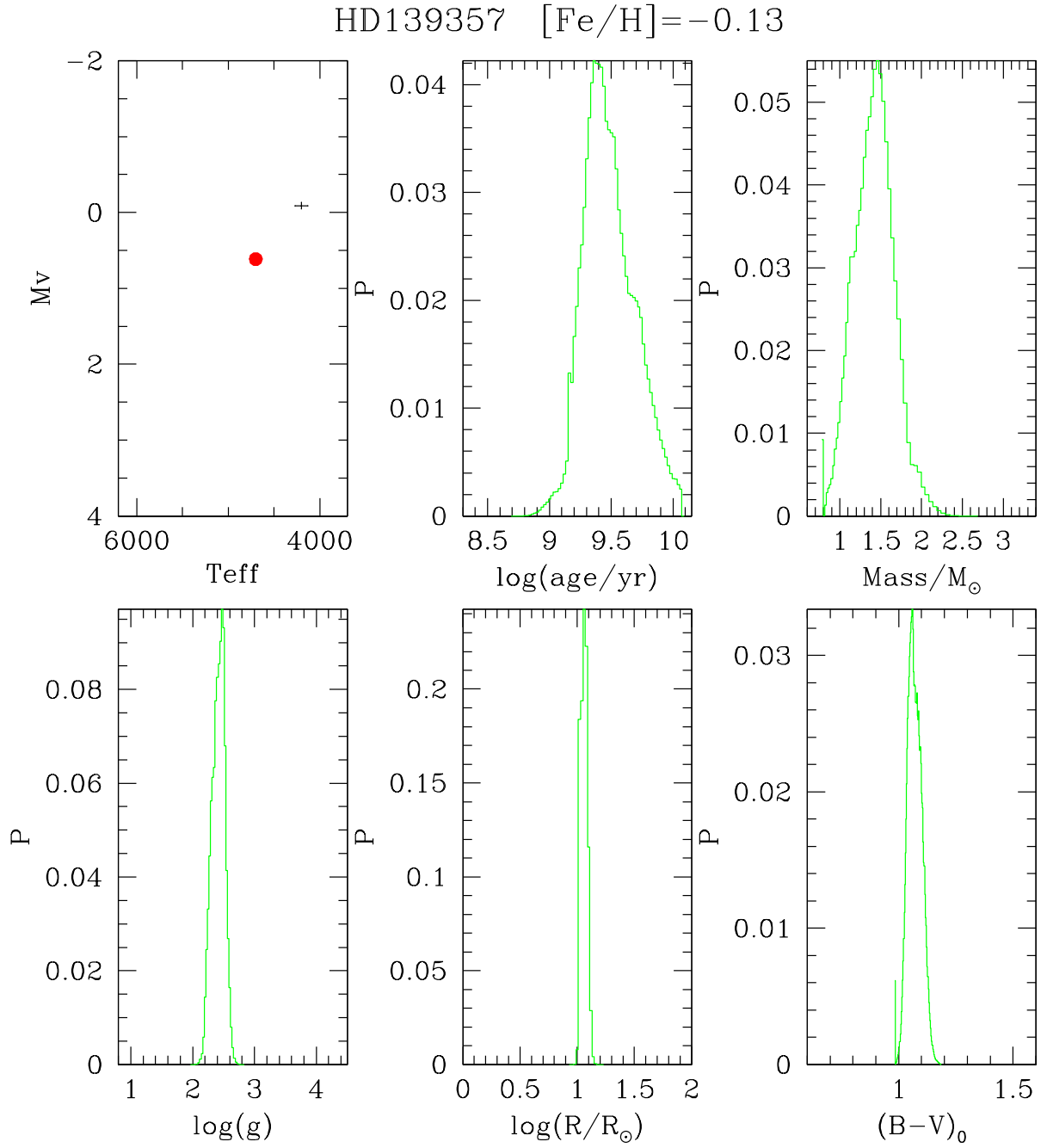


Fig. 8. Stellar parameters of HD 139357. The properties of the host star are listed in detail.

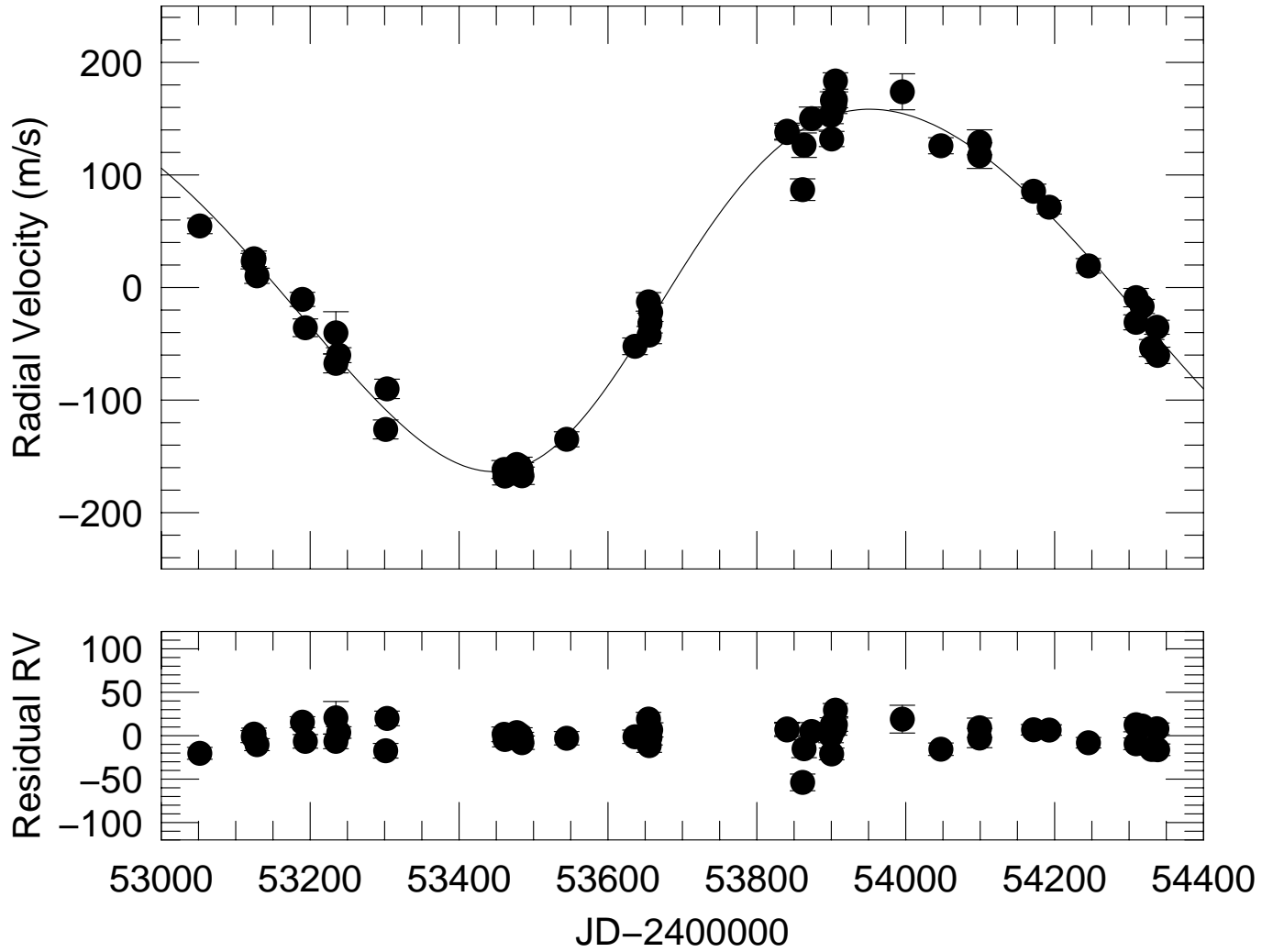


Fig. 9. Radial velocity measurements and RV residuals for HD 139357.

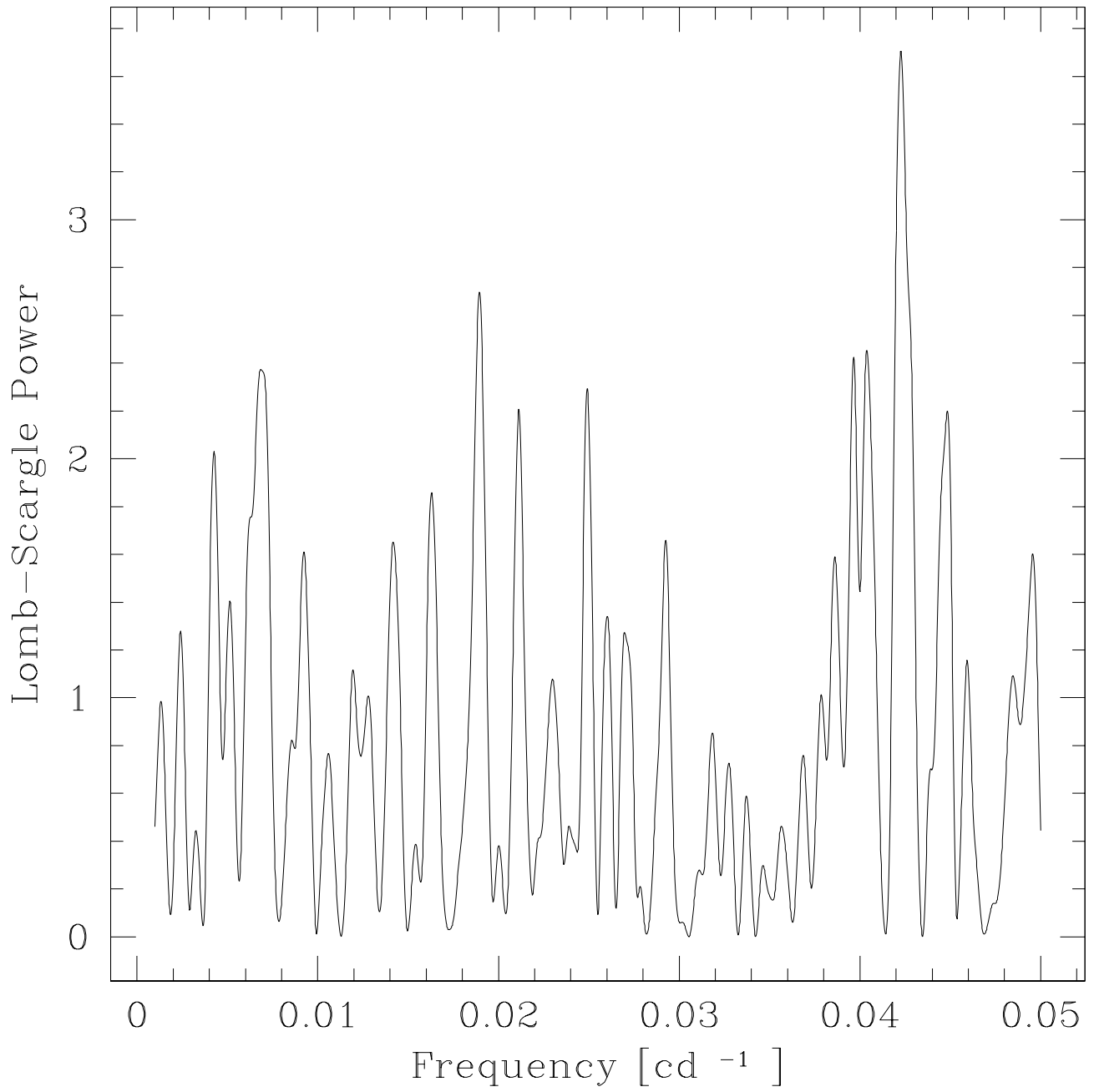


Fig. 10. Lomb-Scargle periodogram of the *HIPPARCOS* photometry for HD 139357.

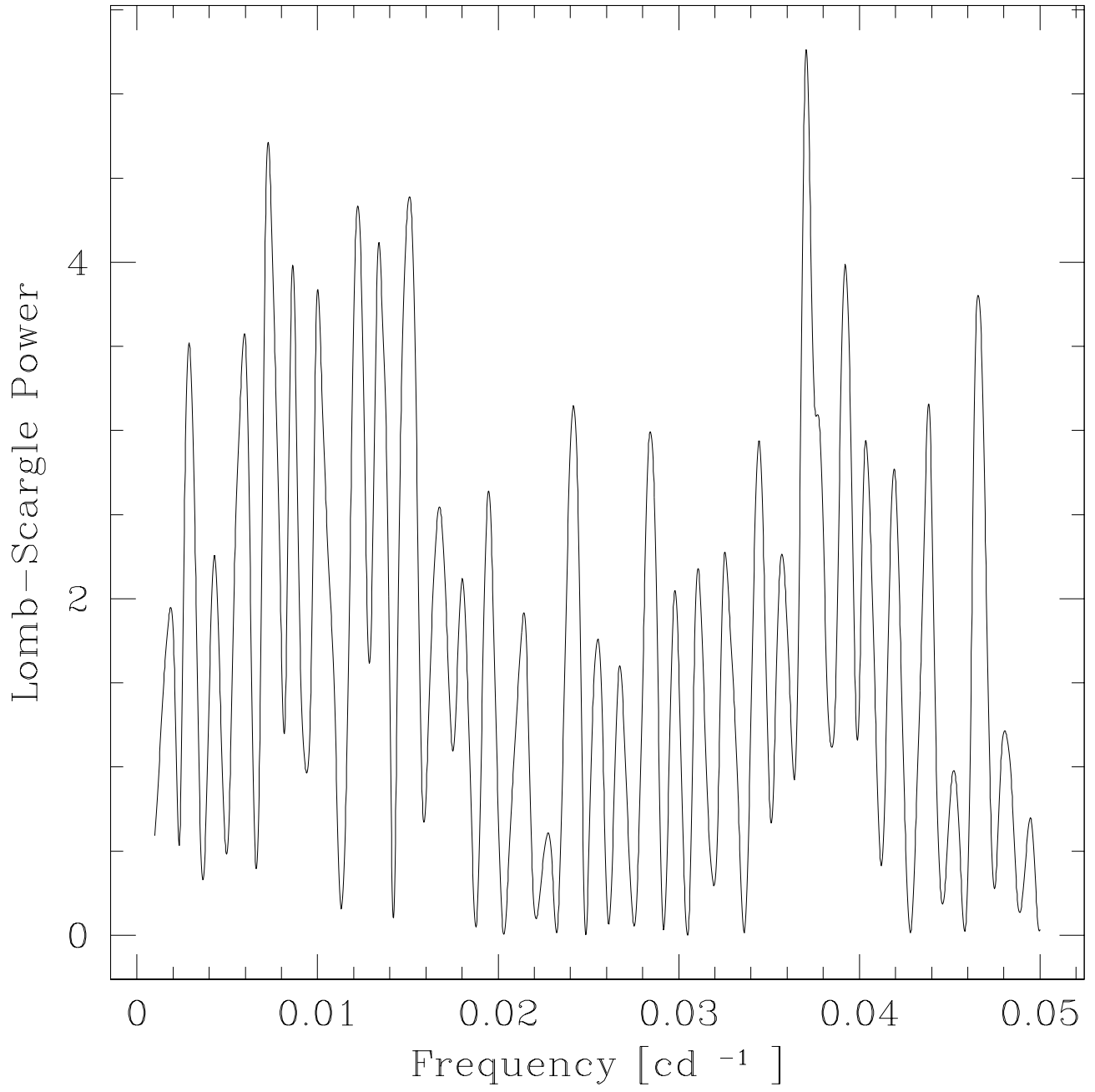


Fig. 11. Lomb-Scargle periodogram of the H α variations for HD 139357.